NASA CR-112047

HEAT TRANSFER DISTRIBUTION ON A DISCONTINUOUSLY CONVECTIVE COOLED SURFACE

by

Renzo Piva† and Richard Poch††

* The work reported herein was supported by the National Aeronautics and Space Administration, under Grant No. NGR-33-016-131

† Visiting Adjunct Professor, New York University Aerospace Laboratory (Assistant Professor of Aerodynamics, University of Rome, Italy)

†† Research Assistant, New York University Aerospace Laboratory

TABLE OF CONTENTS

FOREWORD

This report was prepared under the National Aeronautic and Space Administration, under Grant No. NGR-33-016-131. This grant supports research involving the problem of engine airplane integration and cooling. The authors wish to thank Dr. Antonio Ferri for suggesting this research and for his guidance during the progress of the investigation; and Carlos De Jesus for his helpful collaboration.

ABSTRACT

An active cooling scheme in which discrete cooling passages are used has been investigated. In this scheme, the coolant passages are placed perpendicular to the main stream direction. Streamwise temperature oscillations result from the highly cooled regions, near the coolant channels, being next to regions not directly cooled between the channels.

These oscillations are found to be large in practical applications and therefore the wall temperature cannot be assumed constant as is frequently done in preliminary analysis, since the variations produce substantial deviation in the heat transfer rate. If the wall temperature distribution is calculated by the uncoupled internal heat conduction problem, the use of locally similar methods neglecting the wall temperature history introduce significant errors in the heat transfer calculations and therefore in the amount of coolant required.

The accuracy of the heat transfer rate predictions by these approximations is evaluated by means of both experimental and numerical investigations. Experiments were conducted at free stream Mach number of 6 with several cooling passages. Heat transfer measurements were made and corresponding theoretical analysis were performed for comparison in evaluating both local and overall deviations in the heat transfer rate.

1. INTRODUCTION

The need to maintain the surface of an aeronautical vehicle below the maximum allowable temperature of the material used, creates a challenging problem in hypersonic flight within the atmosphere.

One of the promising methods to retain structural integrity under the severe heating of hypersonic flight is the active cooling using the hydrogen as a heat sink to provide the cooling of the airplane (Ref. 1, 2, 3). A continuous cooling along the surface would be the most desirable condition. This cooling would keep the wall at a constant temperature corresponding to the maximum allowable for the material. The heat transfer would then be the minimum possible for the assigned coolant to free stream stagnation temperature ratio.

Active cooling, however, requires the installation of an additional complicated structural system with an associated weight increase penalty. As a compromise of these two divergent requirements to have low structural weight and efficient cooling, discontinuous active cooling of the surface appears to be a practical solution of the problem. This system is based on the use of a finite number of cooling tubes or channels discretely distributed below the surface at some distance apart. The surface temperature is no longer constant in this case and the cooling of the intermediate region is realized through two different phenomena: the internal solid heat conduction; and the cooling of the external airstream in the regions of coolant passages. Two basic cooling configurations should be considered as limiting cases of the various possible geometries: the coolant channels placed per-

pendicular to the free stream flow in one case; and parallel to the free stream flow in the other. An oscillatory wall temperature distribution in the direction perpendicular to the channels is generated by the discontinuous cooling of the surface. The amplitude and period of such a distribution depends on the geometry and material of the surface and on the difference in the external and coolant stagnation temperatures.

The maximum temperature of the oscillations must be maintained below the permissible temperature for the material and consequently a lower average temperature is inevitable for the entire surface. The lower average temperature results in a higher average heat transfer rate and consequently lower cooling effectiveness. The coupled aerodynamic heat conduction problem must be solved in order to find the real heat transfer distribution. For practical purposes in the engineering approach the two problems are assumed uncoupled and therefore are solved independently. The uncoupling consists of solving successively the two problems and generally a temperature distribution is assumed or calculated from the heat conduction problem and then the corresponding heat transfer rate is determined by the aerodynamic problem. For compressible turbulent boundary layer locally similar methods are usually considered appropriate to calculate the heat transfer for a known wall temperature distribution. In these methods only the local values of the physical properties are considered.

The history of the boundary layer is not taken into account although it may have a very significant influence especially in the presence of large wall temperature gradients. The intention of this study is to examine from a critical point of view the validity in this case of the hypothesis made in

uncoupling the aerodynamic and heat conduction problem and in particular to evaluate the consequent error that may be introduced from:

a) the heat transfer calculation by a locally similar method for the assigned temperature distribution; or

b) the assumption of a temperature distribution that, for lack of a better knowledge, is usually taken to be constant and equal to the maximum permissible value.

The purpose of the present study is to investigate the first coolant configuration (coolant channels perpendicular to the free stream) and particularly

a) to determine experimentally the actual temperature and heat transfer distribution

b) to compare such distributions with those predicted by the approximate methods used in designing the cooled structures, and by more accurate numerical analysis

c) to suggest better geometrical arrangements of the cooling system as a consequence of the above investigation.

Both experimental and numerical approaches were used to obtain a better understanding of this problem. The investigation of the other cooling configuration, that is the one with the cooling passages parallel to the main stream flow direction, will be the object of a subsequent report. In the latter configuration, mixing between the different temperature adjacent streams in the external flow, has an important role. In fact, large temperature oscillations may be significantly attenuated by the mixing phenomena with the result of a larger cooling effectiveness.

2. EXPERIMENTAL INVESTIGATION

A) Experimental Equipment

The Mach 6 blowdown wind tunnel at the N.Y.U. Aerospace Laboratory was utilized. The wind tunnel has a test section with a 12" diameter. For this series of experiments, the stagnation pressure was maintained at about 2000 psia and the stagnation temperature kept at about $900^{\circ}R$ with corresponding Reynolds number about 3×10^{7} per foot. The coolant was air cooled by liquid nitrogen. The coolant temperature was maintained in the range of $250\text{-}350^{\circ}R$.

B) Model

A cylindrican body was used for testing (Figs. 1 and 2). The model is attached to a center body which extends beyond the nozzle in order to avoid three-dimensional effects, and to build up the boundary layer thickness to the same order of magnitude as the distance between the coolant channels (in order to more closely simulate the real flight configuration). All tests have been conducted with a model (Fig. 3), which has five internal circumferential cooling channels situated perpendicular to the flow. Each channel has a coolant flow cross-sectional area of 0.093 $in.^{2}$. Each one is located 2" apart. A 0.030" thick stainless steel shimstock is used as the surface of the cylinder. The continuous thin shimstock was used to have a high thermal resistance surface between the coolant channels; high temperature gradients are thus obtained along the wall during the precooling of the model. In this way at the beginning of the test when all quantities are measured, the mainstream flow is in presence of an oscillatory wall temperature distribution.

Larger distances between coolant channels were obtained by disconnecting certain cooling channels. Different coolant mass flows were also used to have different stagnation temperature ratio between coolant and external flows.

C) Measurements

In addition to monitoring tunnel conditions such at T_o, P_o and P_s, thermocouples are located as shown in (Fig. 4) on the inside surface of the shimstock skin. These thermocouples were used to experimentally determine the heat transfer to the body, as well as the wall temperature distribution on the surface. In addition a motor driven boundary layer probe was used in a few tests to determine the initial boundary layer profiles to be adopted as initial profile for the numerical calculations. All data were recorded on an osillograph used for data reduction.

3. ANALYSIS OF THE HEAT TRANSFER RATE

Heat transfer on the wall is determined by the transient method from the measurement of the slope of the temperature with respect to time. If the shimstock skin is thin and all the other sources of heat transfer are negligible, the aerodynamic heat transfer can be calculated from the temperature increase, assuming that each element of the skin, to which the thermocouple is attached, behaves like a calorimeter. That means that the heat balance is simply

$$\rho c \delta \frac{\partial T}{\partial y} = qa$$

In the present model the shimstock skin is thin but is discontinuously cooled. This fact results in a possible very high internal rate of heat conduction.

If the steady state condition is attained during precooling, however, the increase is almost exclusively due to the aerodynamic heat transfer. This is so because all other sources of heat transfer already balance each other. Some differences between the measured and the real values of heat transfer persist obviously also in the present case.

Commonly used methods to correct the measured values of heat transfer for various losses (Refs.4-5) are not applicable in this case where large heat conduction is always present inside the shimstock. A complete analysis of the heat transfer on the surface was performed with the intention to simulate numerically the experiments. More precisely the experimental precooling can be simulated, if the correct conditions are assigned, until a steady state condition is attained. Then the experimentally measured values for the film coefficient, assumed constant in time but variable at each point in the surface, are imposed in the numerical program to simulate tunnel running conditions. The wall temperature distribution in time is therefore obtained and from that the heat transfer coefficients can be computed with the same transient technique used for the experimental output.

The differences between the film coefficients resulting from these computations and the film coefficients applied as input in the numerical program, for the correspondent element, are due to the heat losses and were taken as a first approximation for the heat transfer correction.

The resulting heat transfer coefficient distribution takes into account all the important corrections and therefore represents the actual aerodynamic

heat transfer rate.

For the internal heat conduction analysis the following approximations were assumed:

a) the model surface was considered as a flat plate considering that the ratio $(\frac{\delta}{R})$ between the shimstock thickness δ and the radius of the cylinder R is very small.

b) the heat transfer coefficient was assumed varying only on the longitudinal direction because in the present model the thermocouples are only on the central region of the shimstock and no measurements were possible on the lateral sides.

c) a finite element numerical scheme (Ref. 6) was used and the height of each element was assumed to be equal to the shimstock thickness (Fig. 5)

With these hypothesis, the heat transfer time dependent equation can be written as

$$K\left(\frac{\partial^2 T}{\partial x^2} + \frac{\partial^2 T}{\partial y^2}\right) = c\rho \frac{\partial T}{\partial t} + \dot{Q}r + \dot{Q}c$$

where $\dot{Q}_R$ is the radiation heat transfer and $\dot{Q}c$ is the convective heat transfer. The last term is natural convection on both the external and internal sides of the shimstock, during the precooling, while it represents forced convection on the external side, on testing conditions.

The corresponding finite difference equation and boundary conditions are reported together with the method of solution in Appendix I. Temperature distribution patterns in time of a simulated test are presented (Fig. 6) for selected elements of the shimstock. The correction term values were found to

be small (from 1% to 7%) at the starting tunnel time, as was predicted, because of the steady state precooling condition. The values are slightly variable in dependence of the temperature and film coefficient distribution and the position on the surface as is shown in (Fig. 7) for the simulated test conditions.

4. EXPERIMENTAL RESULTS AND COMPARISON WITH THEORY

Some of the experimental results are shown in (Figs. 8 to 14). Different coolant temperatures and coolant channel distances resulting in different temperature gradients characterize the different tests.

From the experimental analysis large amplitude of the wall temperature oscillations were found depending on the difference in the external to coolant stagnation temperatures, and on the distance between coolant tubes. In addition to the longitudinal temperature oscillations, transverse wall temperature gradients appear in the present cooling scheme introducing another possible source of errors in estimating the total heat transferred to the panel. These gradients are usually much smaller than the longitudinal ones and their influence on the heat transfer may be neglected. In the present experiments, the few measurements along the two lateral lines of thermocouples (Fig. 4) indicate the negligible value of the transverse gradients and thus the uniformity of the heat transfer in the immediate vicinity of the central line measurements. The amplitude of the longitudinal osicllations may be larger in real flight conditions than those found in the present test conditions, therefore, the wall temperature cannot be assumed constant as is usually done for practical calculations since the variations produce significant deviations in the heat transfer rate. The maximum allowable temperature for the material is usually

considered in the heat transfer calculations. With the above assumption, for the wall temperature distributions characteristic of the experiments conducted, the total heat transfer values are on the order of 15-20% less than the integral of the measured values.

If a more accurate approximation is required, the temperature distribution must be assumed oscillatory or calculated by the incoupled internal heat conduction problem. In this case, the use of locally similar methods, neglecting the wall temperature history, introduces significant errors in the heat transfer calculations. The heat transfer based only on the local properties and calculated with the experimental temperature distribution, shows considerable differences when compared with the experimental results. These differences are due to the downstream influence of the upstream conditions. The history of the boundary layer affects the results in two ways:

a) small scale

b) large scale

The small scale effect is associated with the "between tubes" differences in temperature resulting in large temperature gradients. The experimental heat transfer is higher than the locally similar value in the low temperature regions and lower in the high temperature regions. The differences between the results is dependent on the temperature gradient along the wall, being larger when the temperature gradient is larger. The large scale effect is associated with the different conditions existing for the previous coolant regions. This effect could be more pronounced for rapidly varying external conditions as in the presence of pressure gradients. In the present experiments the large scale effects are essentially due to the fact that the

cooled surface region is inserted between noncooled surface bodies (see Fig. 2). In this case the large scale effect decreases downstream and an asymptotic condition is reached, in which only small scale effects are important. Among the locally similar methods the Spalding Chi method (Ref. 7) was used for comparison. Few tests without cooling (Fig. 8) were done in order to calibrate the above method of calculation to the present case. A disagreement by a factor of 1.06, was found. This difference was eliminated in the comparison, in order to separate the constant error for the physical variations, object of the present study. The local differences in heat transfer are of the order of 10-20% depending on the local value of the temperature gradient (Figs. 8 to 14).

The initial conditions for the cooled surface (large scale) affect substantially a length corresponding to two channels. After this distance, the asymptotic condition is reached. The heat transfer coefficient distribution for few representative tests is reported in (Figs. 15 to 17). From these results it appears that the heat transfer coefficient (or Stanton number), after the asymptotic condition is reached, oscillates around the local similar value and the average error is near zero. Nevertheless, the total heat transfer is larger, and to prove that, the following restrictive approximations can be written:

$$\int_o^L \Delta h\ (x)\ dx \simeq 0$$

where $\Delta h\ (x)$ is the difference in h between the experimental and locally similar values. Since the heat transfer is

$$\dot{q} = h\Delta T \text{ with } \Delta T = T_o - T_w\ (x)$$

and because ΔT is larger when h is larger

$$\dot{q}_{total} = \int_o^L \Delta\dot{q}\ (x)\ dx > 0$$

where $\Delta \dot{q}(x)$ is the corresponding variation in heat transfer due to the $\Delta h(x)$.

From this result it can be calculated that, also in this restrictive case, the nonsimilar or small scale history effect increases the total heat transfer and the amount depends on the temperature distribution. In the present case this difference is small, on the order of a few percent (2-3%) but it increases with larger temperature differences as encountered in flight conditions. This difference arises as a consequence of physical phenomena, therefore, even if it is small, it must be accounted for. The above results imply that:

a) A larger amount of coolant is necessary to keep the same maximum temperature on the surface, because of the slight but not negligible increase in the amount of the total heat transfer.

b) Larger distances between the channels may be used since the heat transfer is significantly lower in the intermediate regions.

From an engineering point of view, these differences in the heat transfer must be considered in the design of a vehicle and a more accurate method of prediction seems necessary. The numerical method used in (Ref. 8) predicts with greater accuracy the heat transfer distribution for compressible turbulent boundary layers when the boundary layer history effects are significant.

Two cases of this calculation are shown in (Figs. 18-19). The flow conditions are typical of those in the Mach 6 tunnel used for the present experiments. The boundary layer profile measured in the present and previous experiments (Refs. 8 and 9) was used as an initial condition in the numerical calculations. The wall temperature distribution has a sinusoidal form that simply and with good approximation represents the experimental distribution.

The wall temperature distribution is expressed in the form

$$T_w(x) = T_{wo} + T_{w1} \sin [n\pi(x-x_o)]$$

where T_{wo} is the average wall temperature, T_{w1} is the amplitude of the oscillation, x_o is the initial station and n is an integer that can vary the frequency of oscillations.

In the example reported the previous constant has the values indicated in (Figs. 18-19). With this method, a better prediction of the heat transfer distribution is obtained if the wall temperature distribution is known. A numerical solution that can solve the internal conduction field and the boundary layer coupled would be necessary to predict the heat transfer distribution. Only the surface data and the coolant and flight conditions would be needed as inputs, but this calculation would be very cumbersome and computer time consuming.

5. CONCLUDING REMARKS

The calculation of the heat transfer for discontinually active cooled surfaces with oscillatory wall temperature distributions have been investigated. A critical analysis of the approximate methods used in the designing of these panels was conducted using both experimental and numerical approaches. From these investigations it can be concluded that:

a) The error introduced by the use of locally similar methods in the heat transfer calculation for an assigned oscillatory temperature distributions is locally large (10-15%). The

error in the integral value is however considerably smaller (2-3%) because of the opposite signs of the local errors.

b) A larger error (20%) in the integral value of the heat transfer is introduced by the assumption that the wall temperature is constant and equal to the maximum permissible value for the material used.

In fact the temperature oscillation are found to be very large and, therefore, the wall temperature cannot be assumed constant.

The above results suggest that in comparison with the values computed by the approximate methods:

a) A larger amount of coolant is necessary in order to keep the same maximum temperature on the surface.

b) A larger distance between the channels is allowable since the heat transfer is significantly lower in the intermediate regions.

A more complete experimental investigation would be necessary to correlate the results and prescribe some engineering formulas to correct the heat transfer prediction by the approximate methods.

NOMENCLATURE FOR APPENDIX

A_i	Surface area of block i (ft^2)
$A_{i,j}$	Area of block i which touches block j (ft^2)
C_p	Specific heat at constant pressure $\frac{BTU}{lb - {}^oR}$
d_i	Length of block i (ft)
h	Heat-transfer coefficient $\frac{BTU}{sec - ft^2 - {}^oR}$
h_j	Joint heat transfer coefficient $\frac{BTU}{sec - ft^2 - {}^oR}$
K_m	Conductivity of surface material $\frac{BTU}{sec - ft - {}^oR}$
Q	Heating rate $\frac{BTU}{sec}$
T	Temperature (^oR)
Δt	Time Interval (sec)
V_i	Volume of block i (ft^3)
W_i	Width of block i (ft)
ϵ_i	Emissivity of block surface
ρ_m	Material density (lb/ft^3)
σ	Stefan-Boltzmann constant $\frac{BTU}{sec - ft^2 - {}^oR^4}$
T_{pi}	Temperature of block i at the beginning of computing interval (^oR)
T_s	Temperature of supporting structure (^oR)
ds	Length of supporting structure (^oR)
T_r	Recovery temperature (^oR)

APPENDIX I

The basic procedure employed in this program requires that the surface configuration be divided into a system of small blocks and described by the inputs, the size, material composition and heat transfer modes for each individual block and the interrelations between the blocks. These inputs are put into the heat-balance equation for the individual blocks and the computer solves the resulting matrix for the temperature of the blocks as a function of time.

The heat-balance equation for each block is:

$$(\dot{Q}_{CONV})_i - (\dot{Q}_{COND})_i - (\dot{Q}_{RAD})_i - (\dot{Q}_{JOINT})_i = (Q_{STORED})_i$$

For convection,

$$(\dot{Q}_{CONV})_i = h_i A_i (T_i - T_{Pi})$$

For conduction,

$$(\dot{Q}_{COND})_i = \sum (\Delta \dot{Q}_{COND})_{i,j}$$

where $(\Delta \dot{Q}_{COND})_{i,j}$ is the conduction between the box in question and the jth box adjacent to it.

$$(\Delta \dot{Q}_{COND})_{i,j} = \frac{2 K_m A_{i,j} (T_i - T_j)}{d_i + d_j}$$

For radiation,

$$\left(\dot{Q}_{RAD}\right)_i = \sigma \varepsilon_i A_i T_{P_i}^4$$

At the joint where the model surface comes in contact with the supporting structure, the conduction between the block and the structure is:

$$\left(\dot{Q}_{JOINT}\right)_i = \frac{2 A_{i,s} \left(T_i - T_s\right)}{\frac{2}{h_j} + \frac{d_i + d_s}{K_m}}$$

For the stored heat

$$\left(\dot{Q}_{STORED}\right)_i = \frac{C_p \rho_m V_i \left(T_i - T_{P_i}\right)}{\Delta t}$$

Substituting these terms into the heat-balance equation gives the following equation for each individual block

$$\left[\frac{2 K_m A_{i,i-1}}{d_i + d_{i-1}}\right] T_{i-1} - \left[2 K_m \left(\frac{A_{i,i-1}}{d_i + d_{i-1}} + \frac{A_{i,i+1}}{d_i + d_{i+1}} + \frac{A_{i,i-10}}{d_i + d_{i-10}} + \frac{A_{i,i+10}}{d_i + d_{i+10}}\right) + \frac{C_p \rho_m V_i}{\Delta t}\right] T_i + \left[\frac{2 K_m A_{i,i+1}}{d_i + d_{i+1}}\right] T_{i+1} + \left[\frac{2 K_m A_{i,i-10}}{d_i + d_{i-10}}\right] T_{i-10} +$$

$$+\left[\frac{2 K_m A_{i,i+10}}{d_i + d_{i+10}}\right] T_{i+10} = h_i A_i \left(T_z - T_{P_i}\right) + \sigma \varepsilon_i A_i T_{P_i}^4 - \frac{C_p \rho_m V_i}{\Delta t} T_{P_i}$$

The surface configuration considered for analysis is illustrated in (Fig. 5). The boundary conditions for this configuration are:

1. There is no heat transfer out of the system in the (x) direction.
2. In the (y) direction the only heat transfer out of the system is Q_{joint}.

Because of the periodic nature of the temperature distribution along the model surface, only one channel was used for the surface configuration. The temperature distribution along any channel is the same as that along this channel. In order to get a fine grid for the surface configuration only one-half the period of the temperature oscillation was used.

REFERENCES

1. Becker, John, V., "New Approaches to Hypersonic Aircraft," ICAS, Rome, Italy, September 14-18, 1970.

2. Flieder, W., Richard, C.E., Buchmann, O.A., and Walters, F.M., "An Analytical Study of Hydrogen Cooled Panels for Application to Hypersonic Aircraft," NASA CR-1650, April 1971.

3. McConarty, William A., and Anthony, Frank M., "Bell Aerosystems Company Report, No. 7305-901001," Bell Aerosystems Company, Buffalo, New York, December 1968.

4. Wilson, Donald, M., "The Predictions of Errors and the Improvement of Data Obtained in Wind-Tunnel Heat-Transfer Tests," NOLTR-70-197, September 24, 1970.

5. Nagel, A.L., Fitzsimmons, H.D., and Doyle, L.B., "Analysis of Hypersonic Pressure and Heat Transfer tests on Delta Wings with Laminar and Turbulent Boundary Layers," NASA CR-535, August 1966.

6. Garrett, Bernard, and Pitts, Joan I., "A General Transient Heat-Transfer Computer Program for Thermally Thick Walls," NASA TM X-2058, August 1970.

7. Neal, Luther, Jr., and Bertram, Mitchel, H., "Turbulent-Skin-Friction and Heat-Transfer Charts Adapted from the Spalding and Chi Method," NASA TN D-3969, May 1967.

8. Liu, T.M., and Piva, Renzo, "Turbulent Boundary Layer Flow with Osillatory Wall Temperature, NYU Report No. 71-24, September 1971.

9. Alzner, E. and Zakkay, V., "Turbulent Boundary Layer Shock Interaction With and With Injection," NYU Report NYU-AA-69-24; also ARL Report No. ARL 70-0092, June 1970.

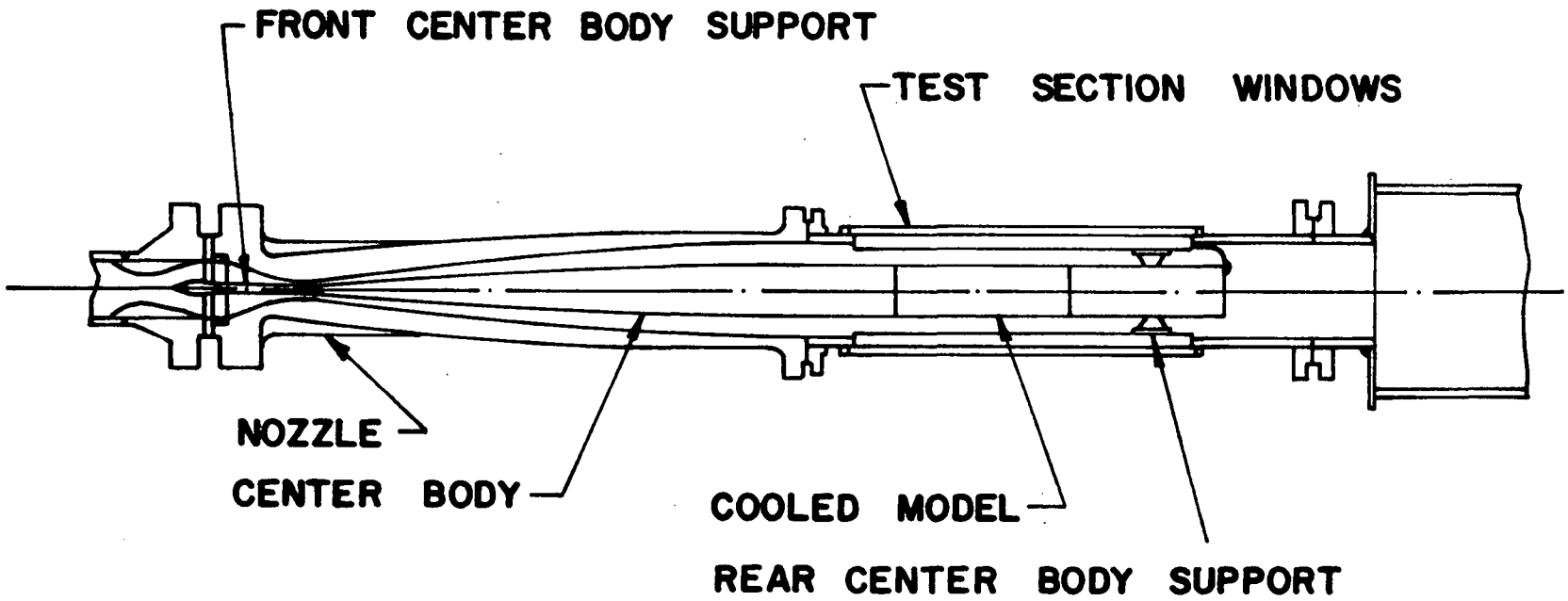

Fig. 1 Cooled model with center body support and test section

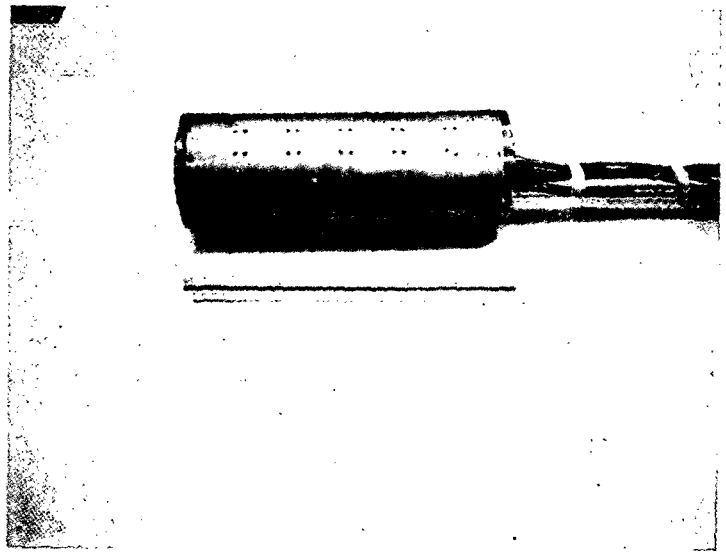

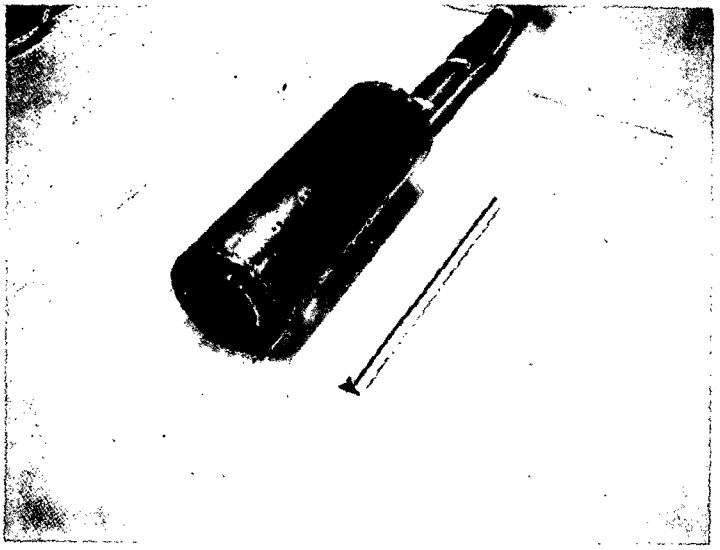

Fig. 2 Experimental Model

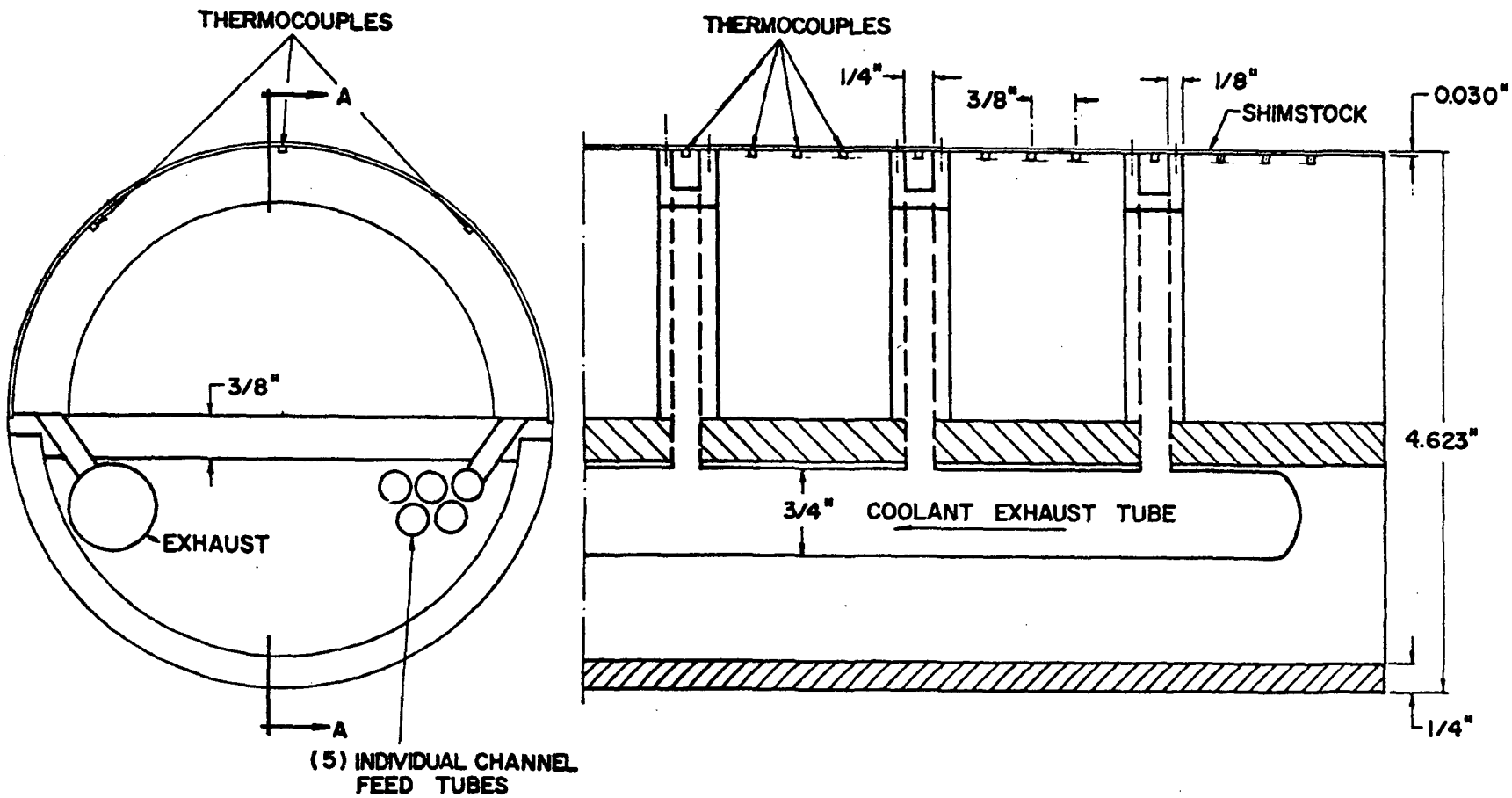

Fig. 3 Experimental model

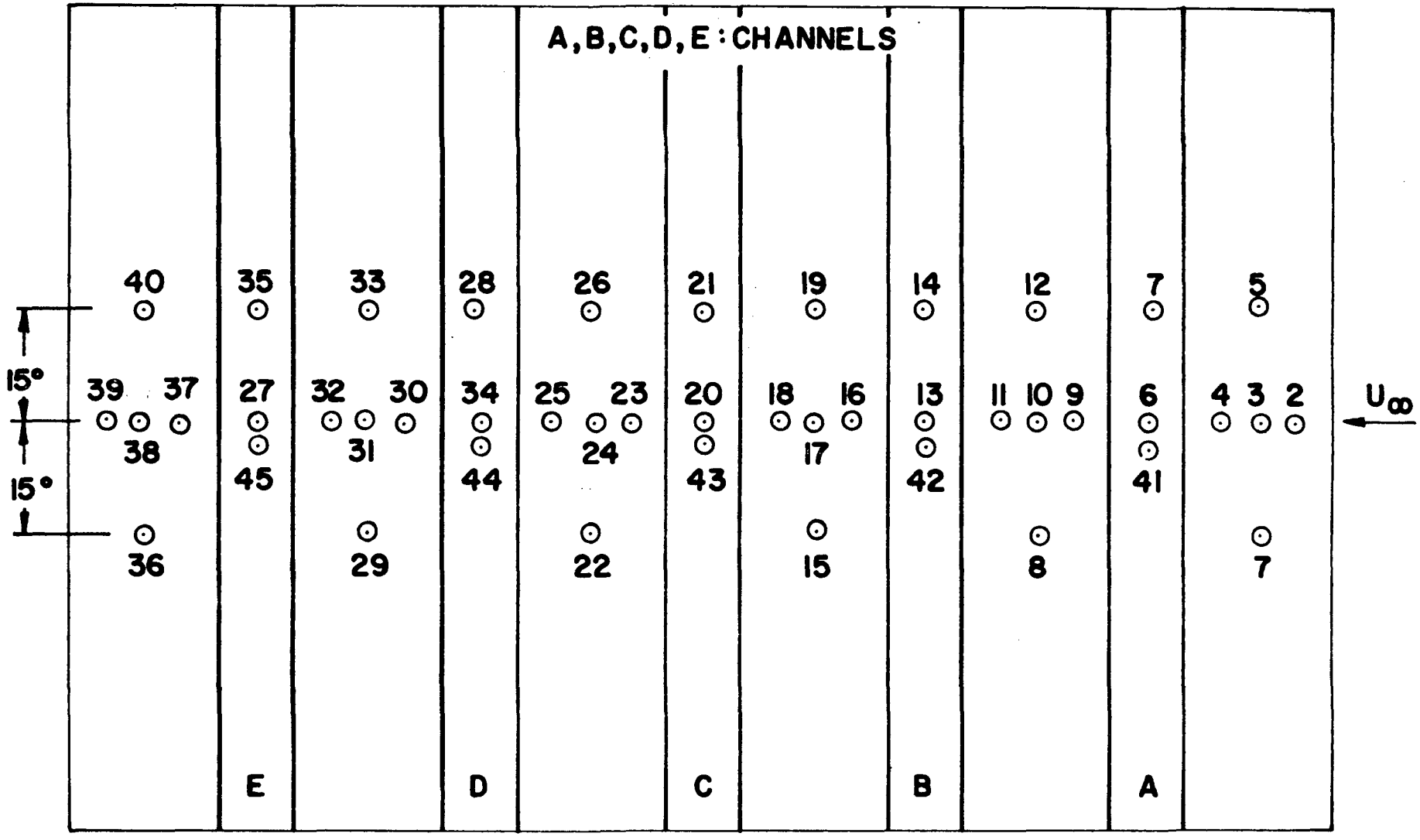

Fig. 4 Thermocouples location on the shimstock

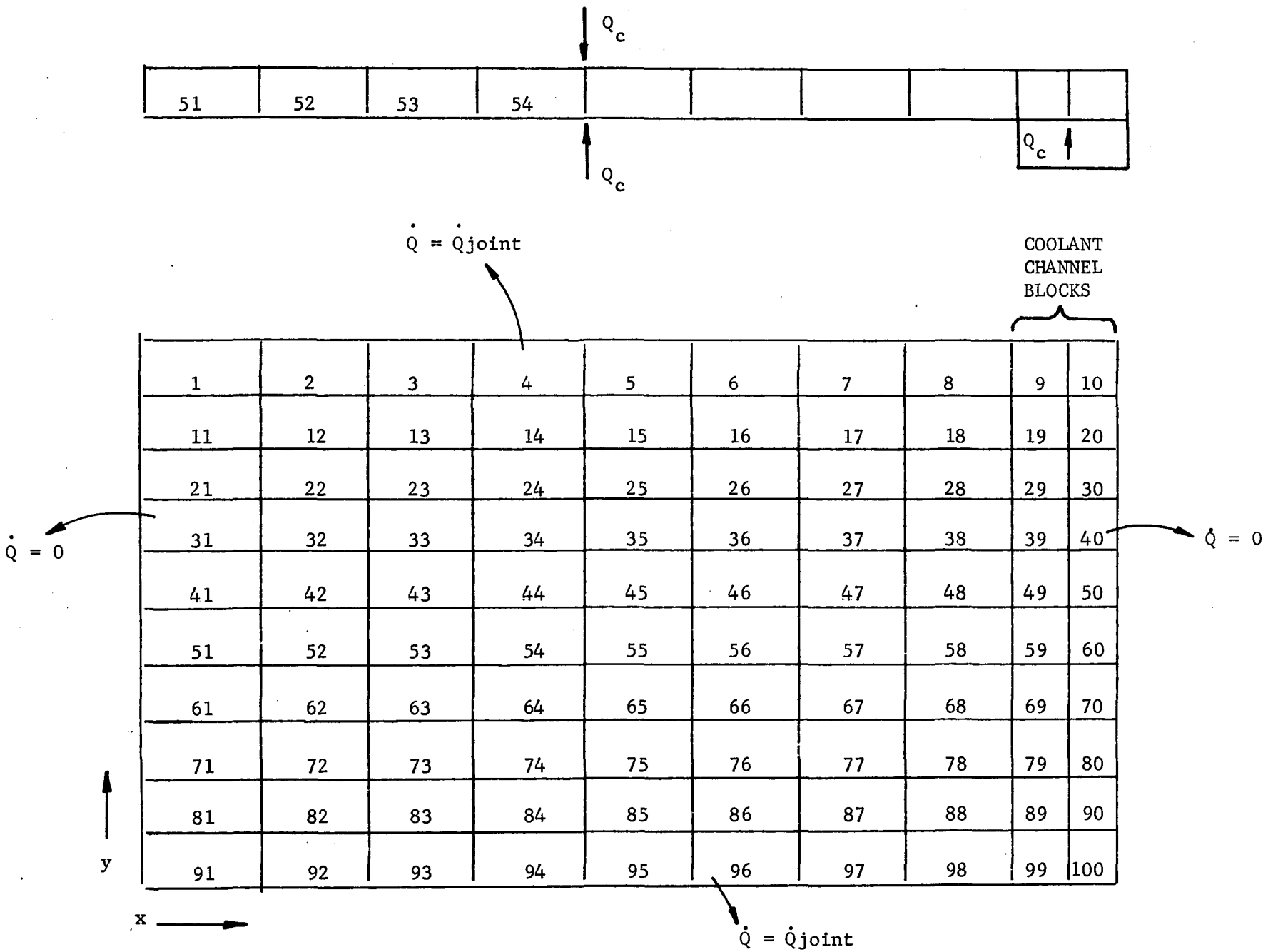

Fig. 5 Surface configuration for computer program

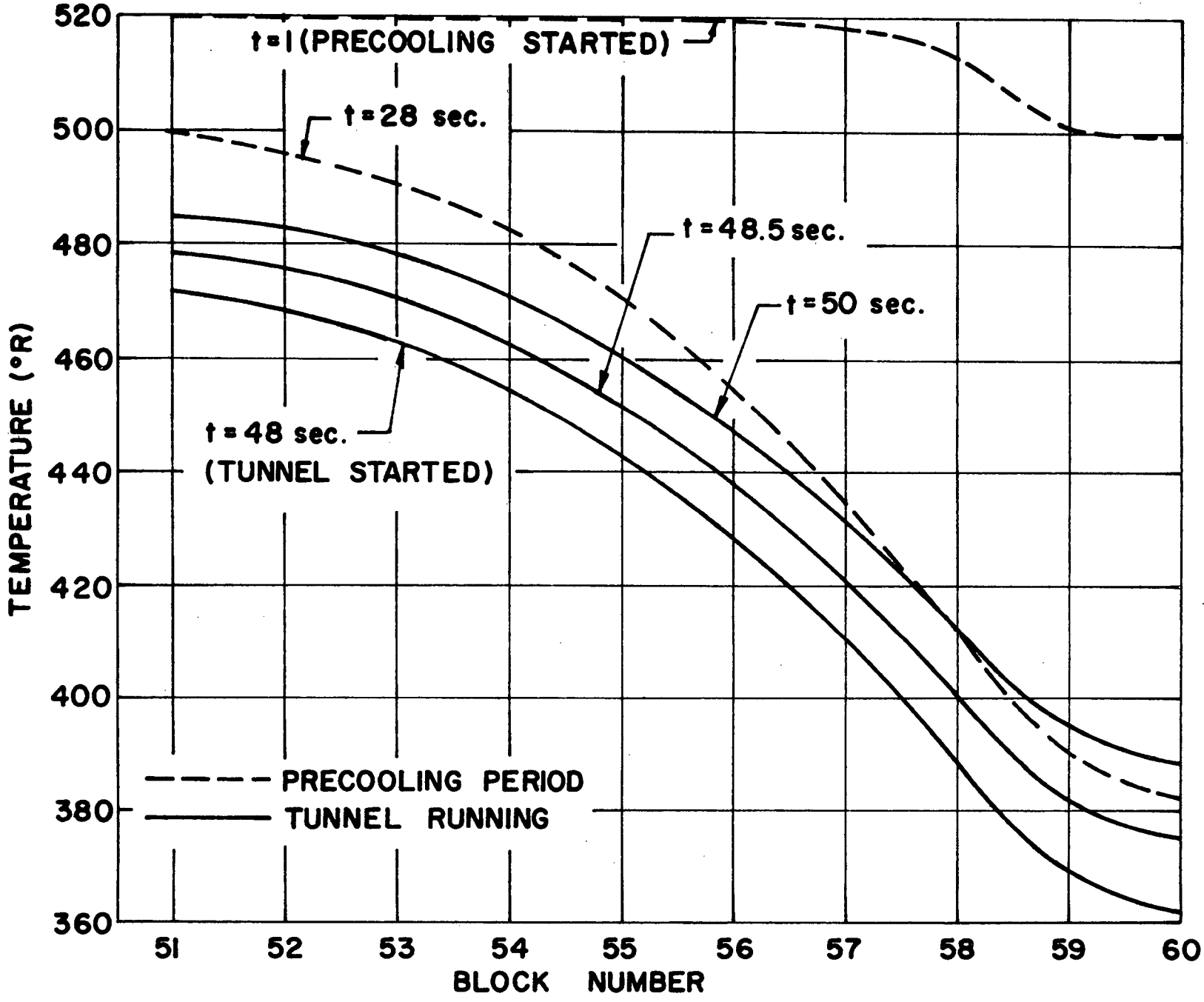

Fig. 6 Temperature distribution as a function of time

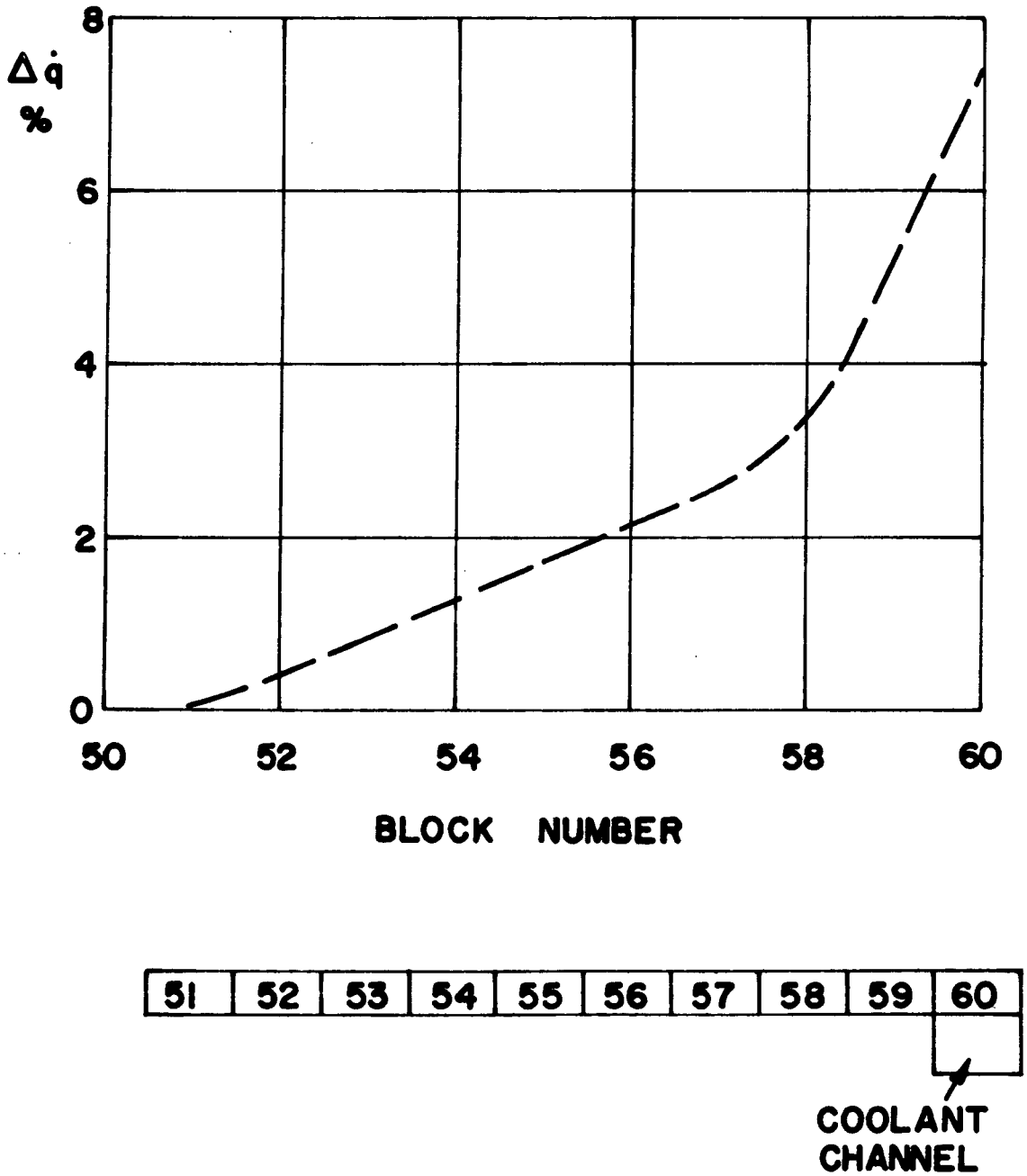

Fig. 7 Conduction correction term distribution from the test numerical simulation

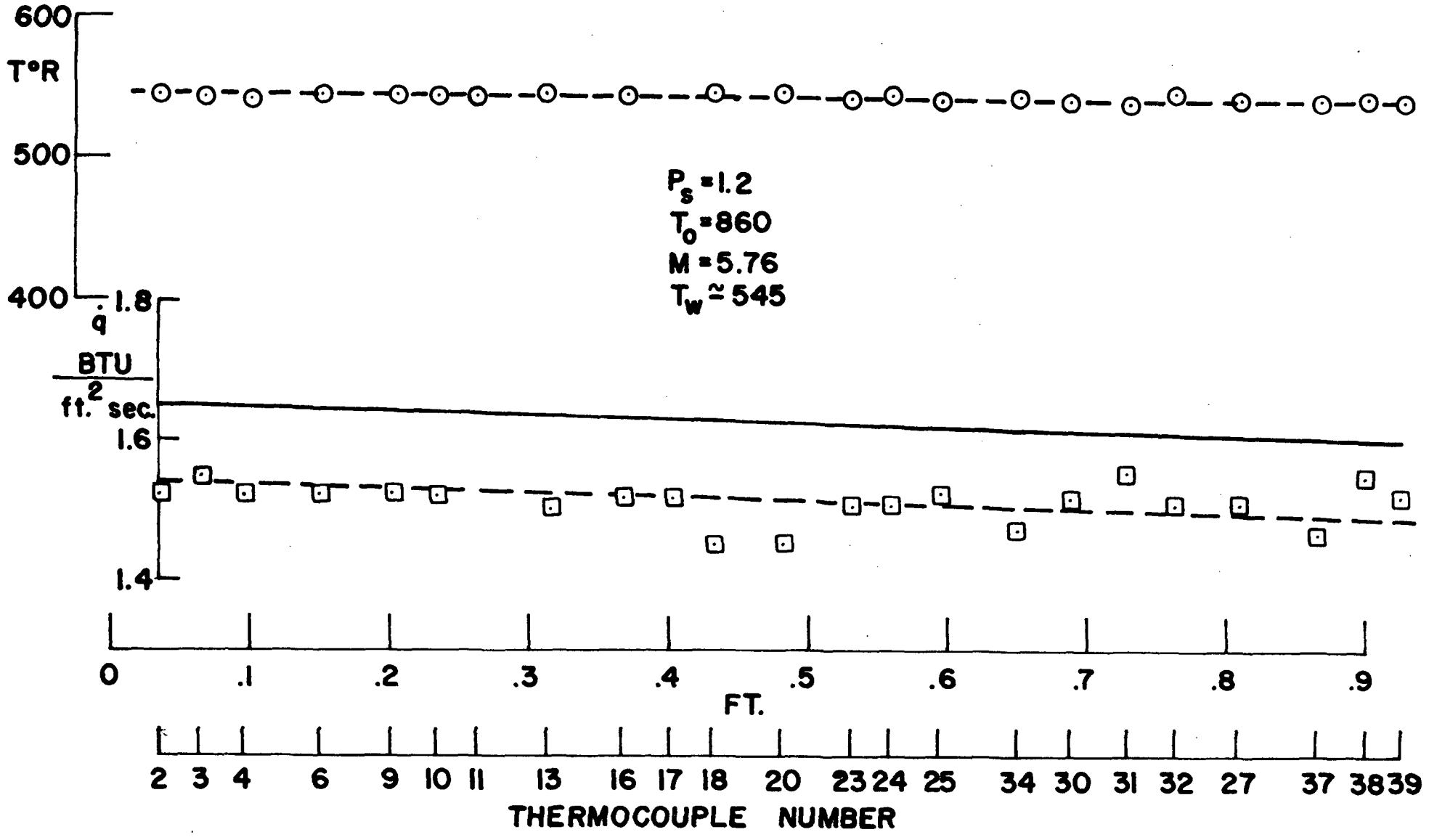

Fig. 8 Heat transfer distribution: no cooling

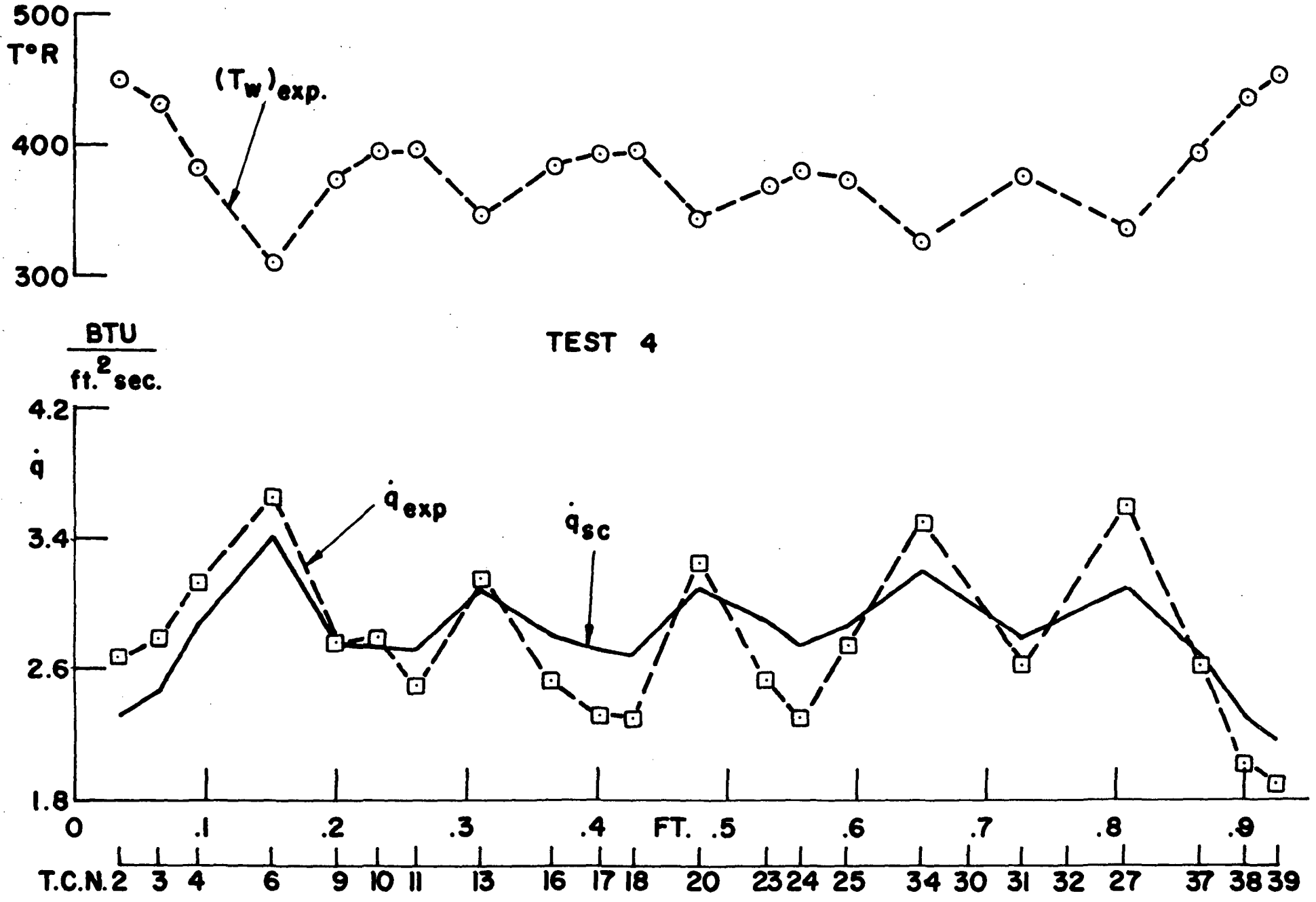

Fig. 9 Temperature and heat transfer distributions: 5 coolant channels

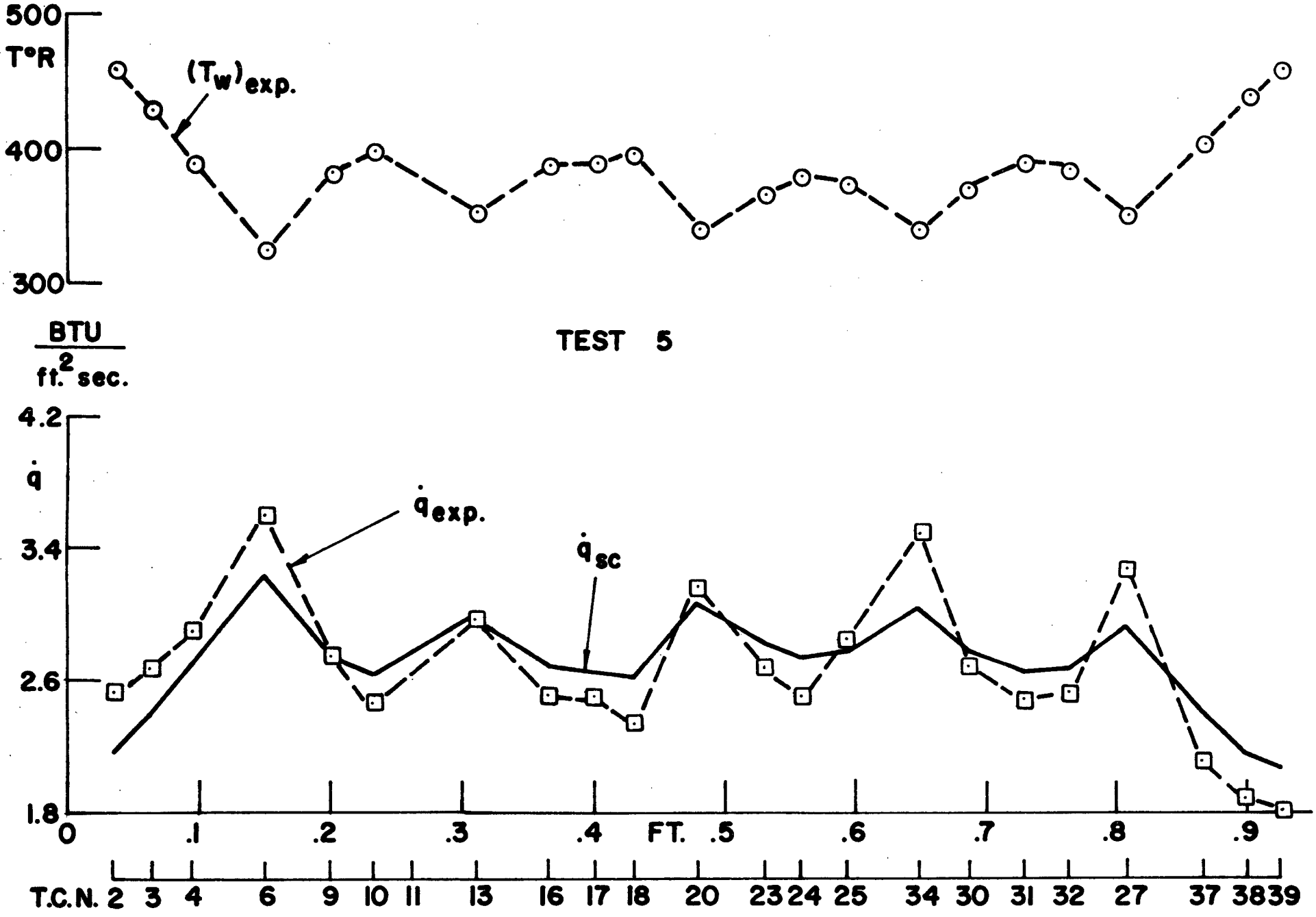

Fig. 10 Temperature and heat transfer distributions: 5 coolant channels

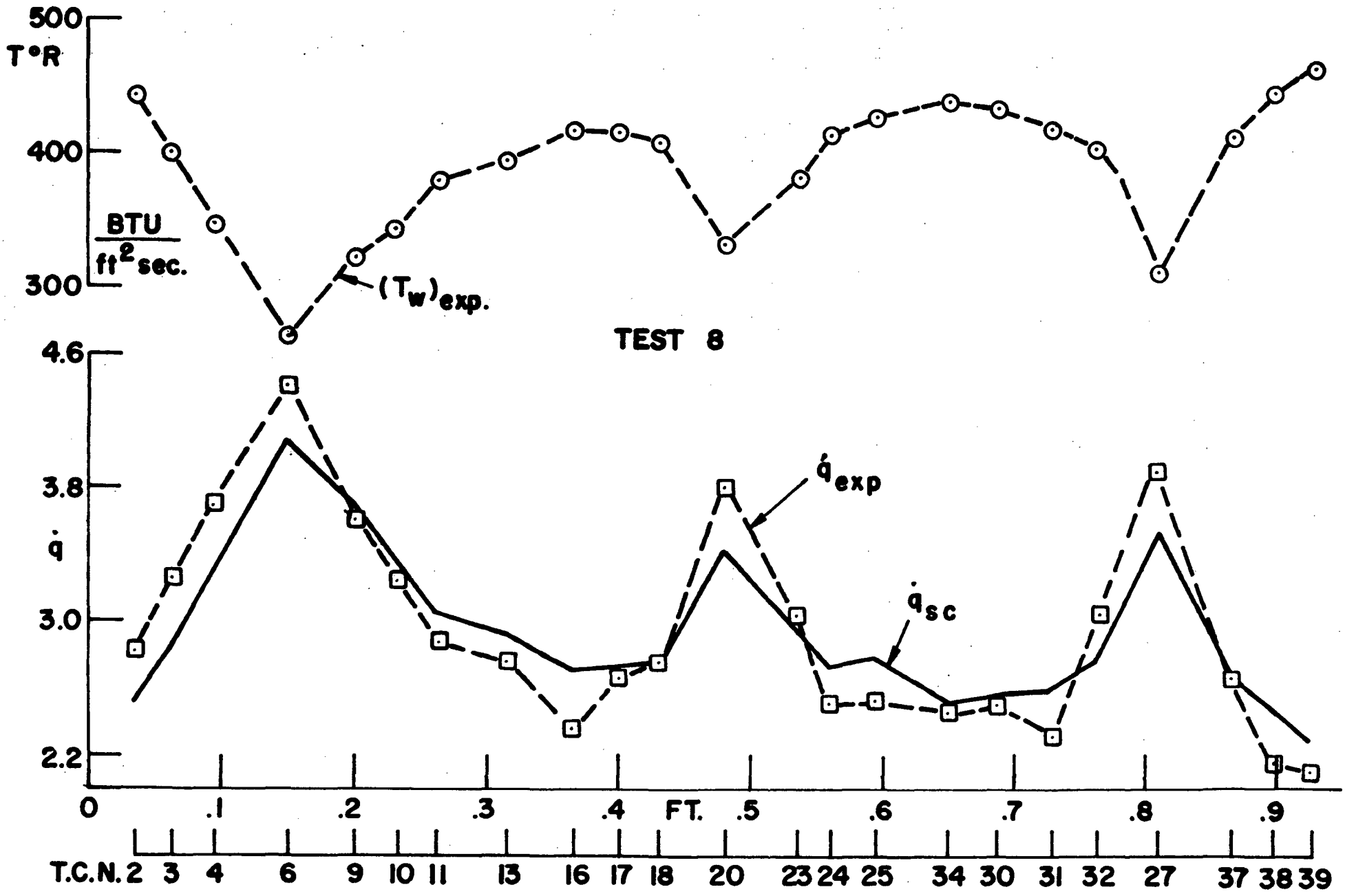

Fig. 11 Temperature and heat transfer distributions: 3 coolant channels

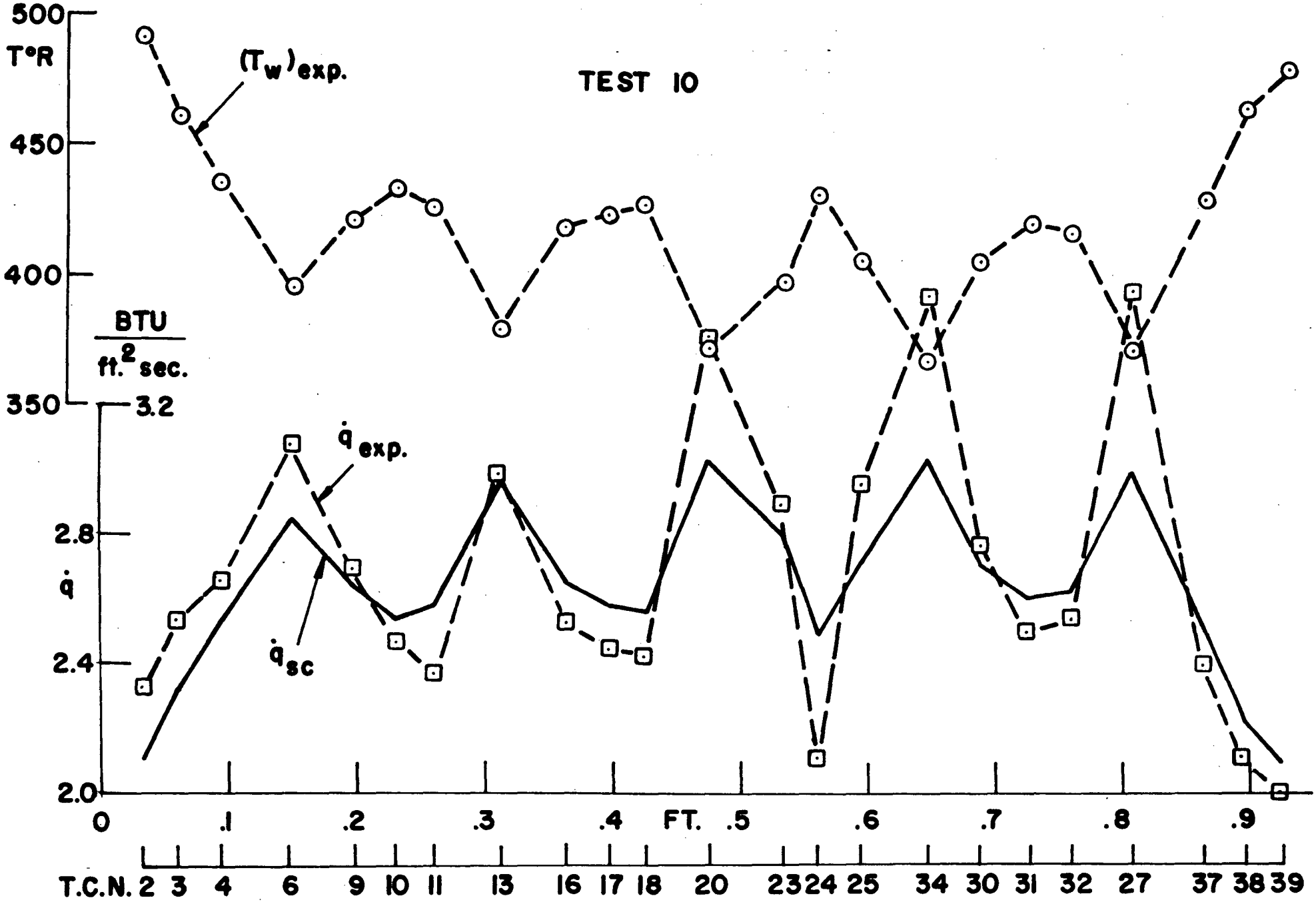

Fig. 12 Temperature and heat transfer distributions: 5 coolant channels

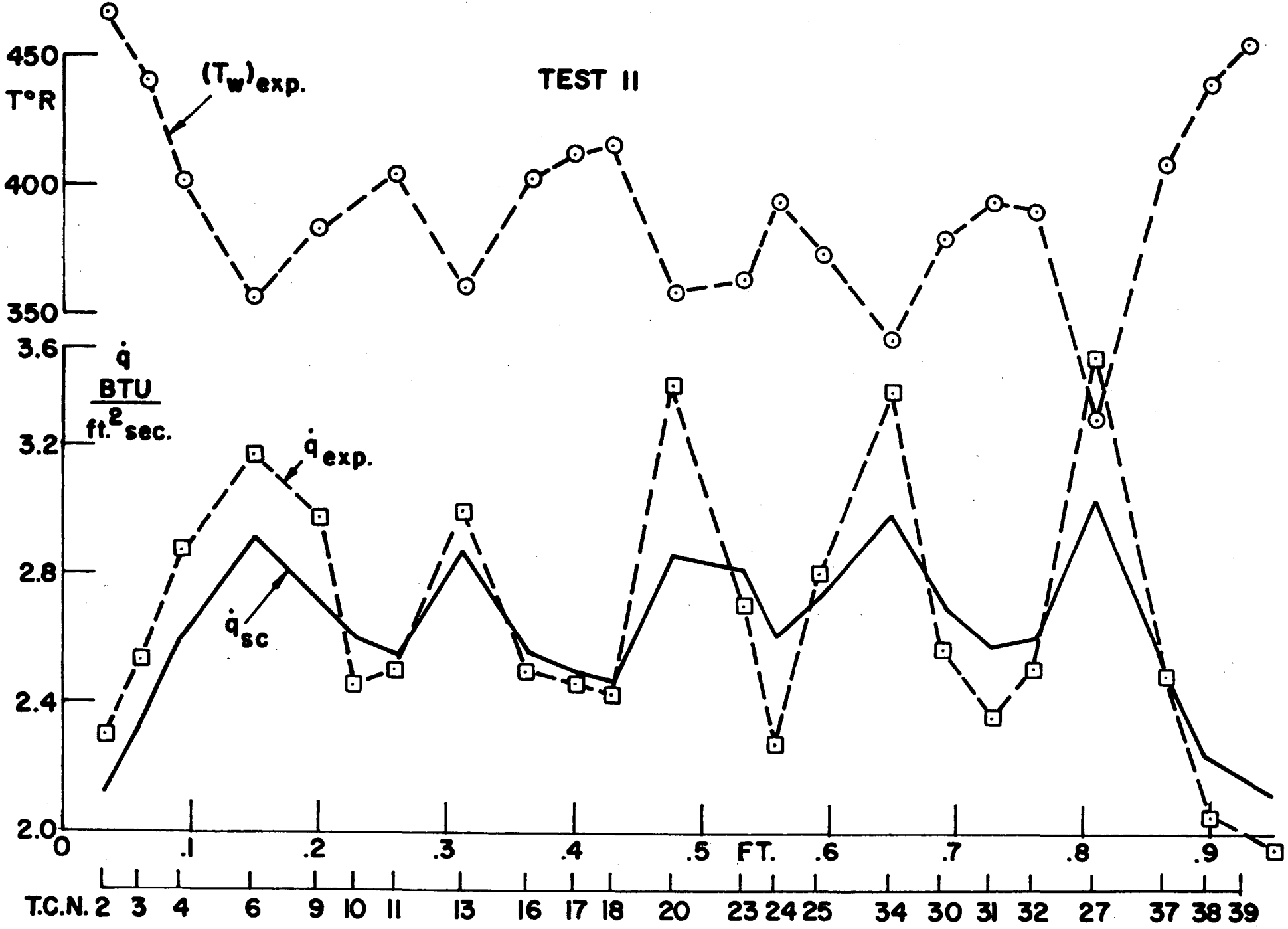

Fig. 13 Temperature and heat transfer distributions: 5 coolant channels

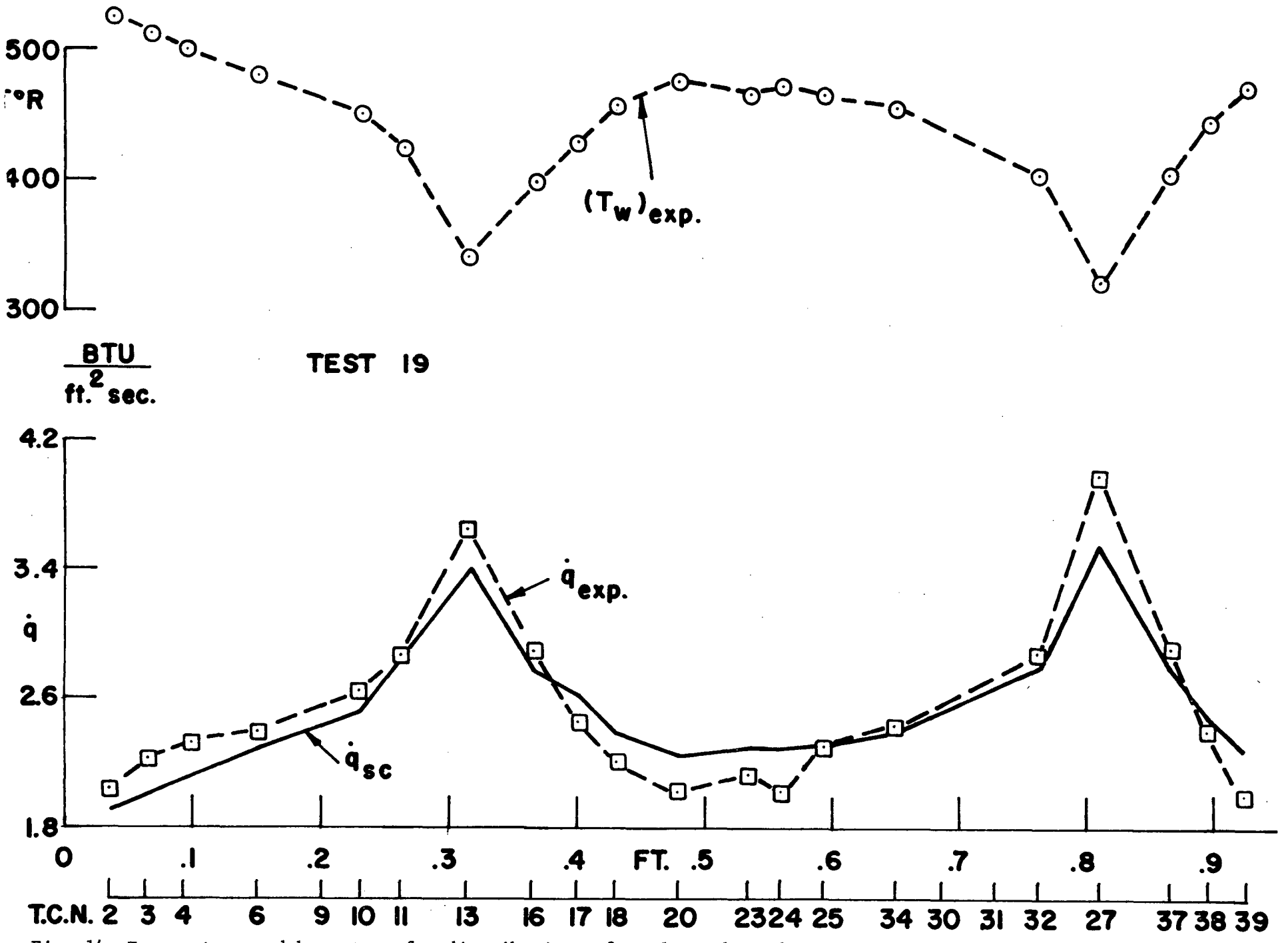

Fig. 14 Temperature and heat transfer distributions: 2 coolant channels

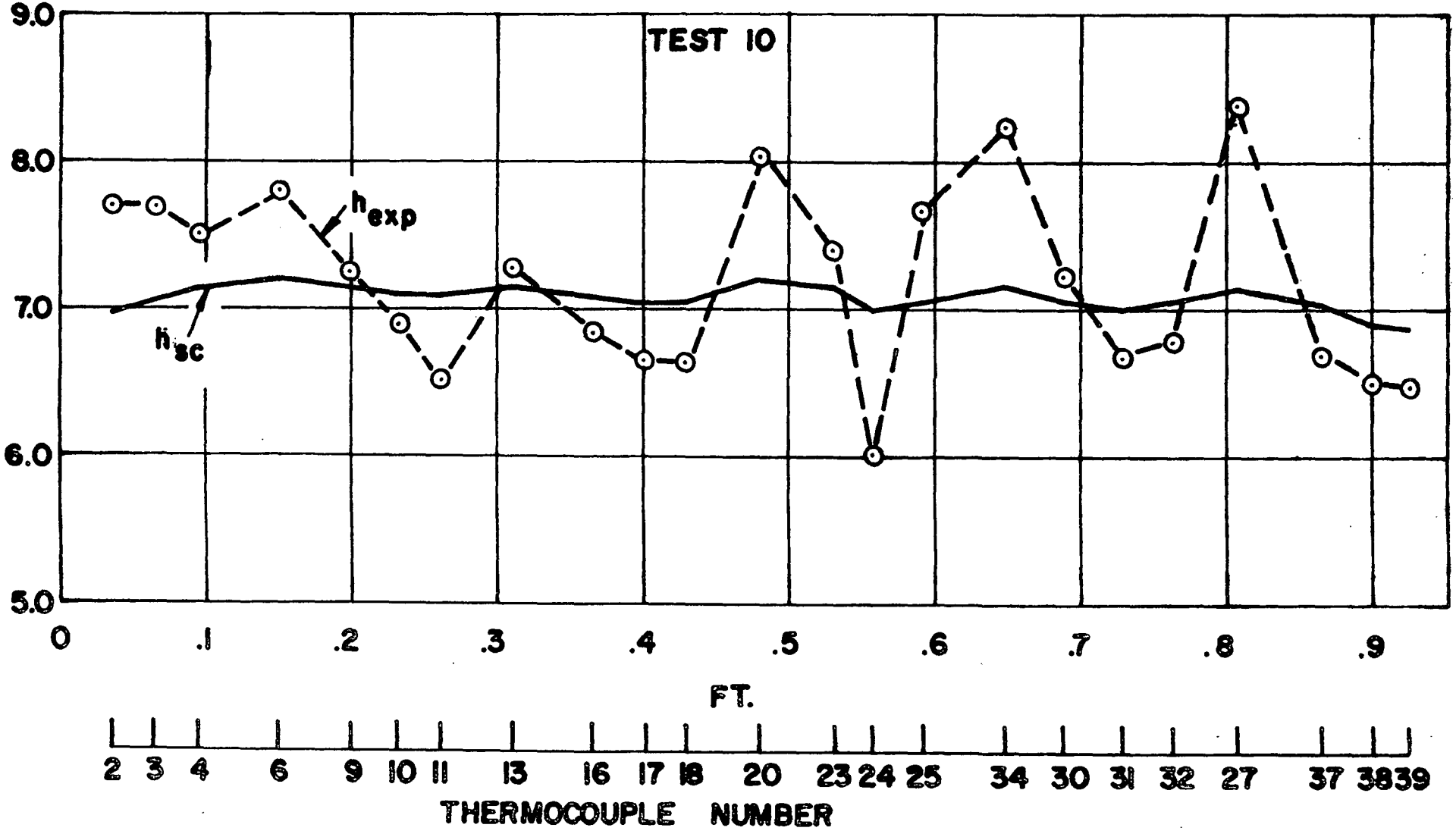

Fig. 15 Heat transfer coefficient distributions

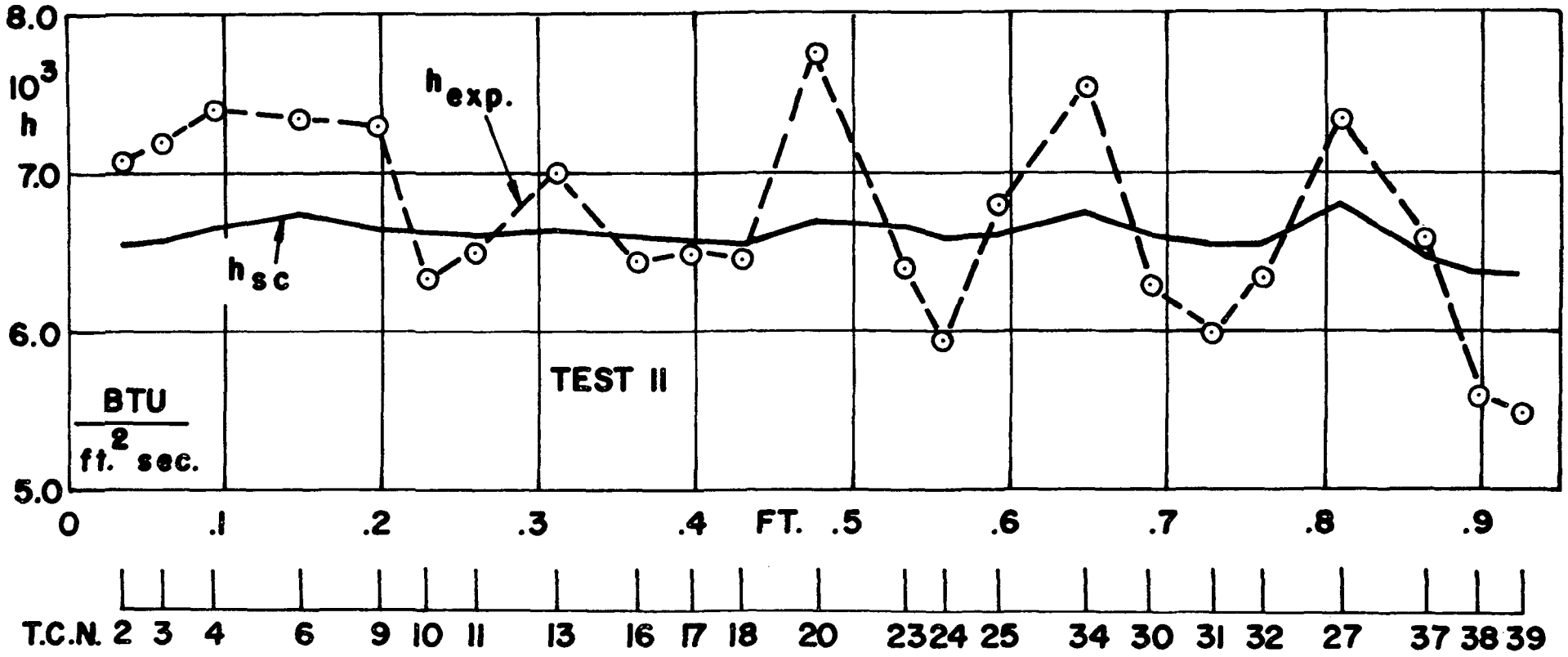

Fig. 16 Heat transfer coefficient distributions

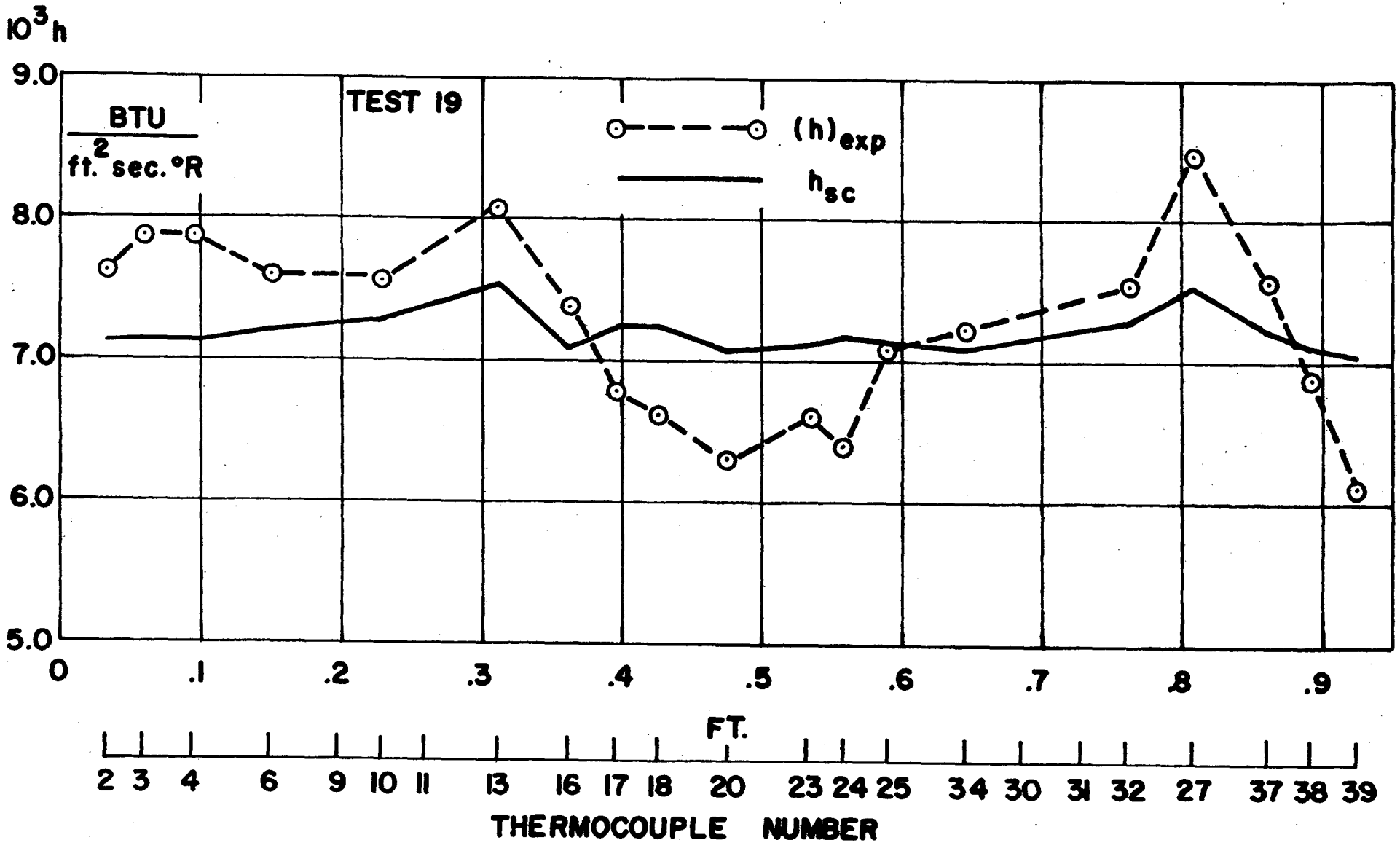

Fig. 17 Heat transfer coefficient distributions

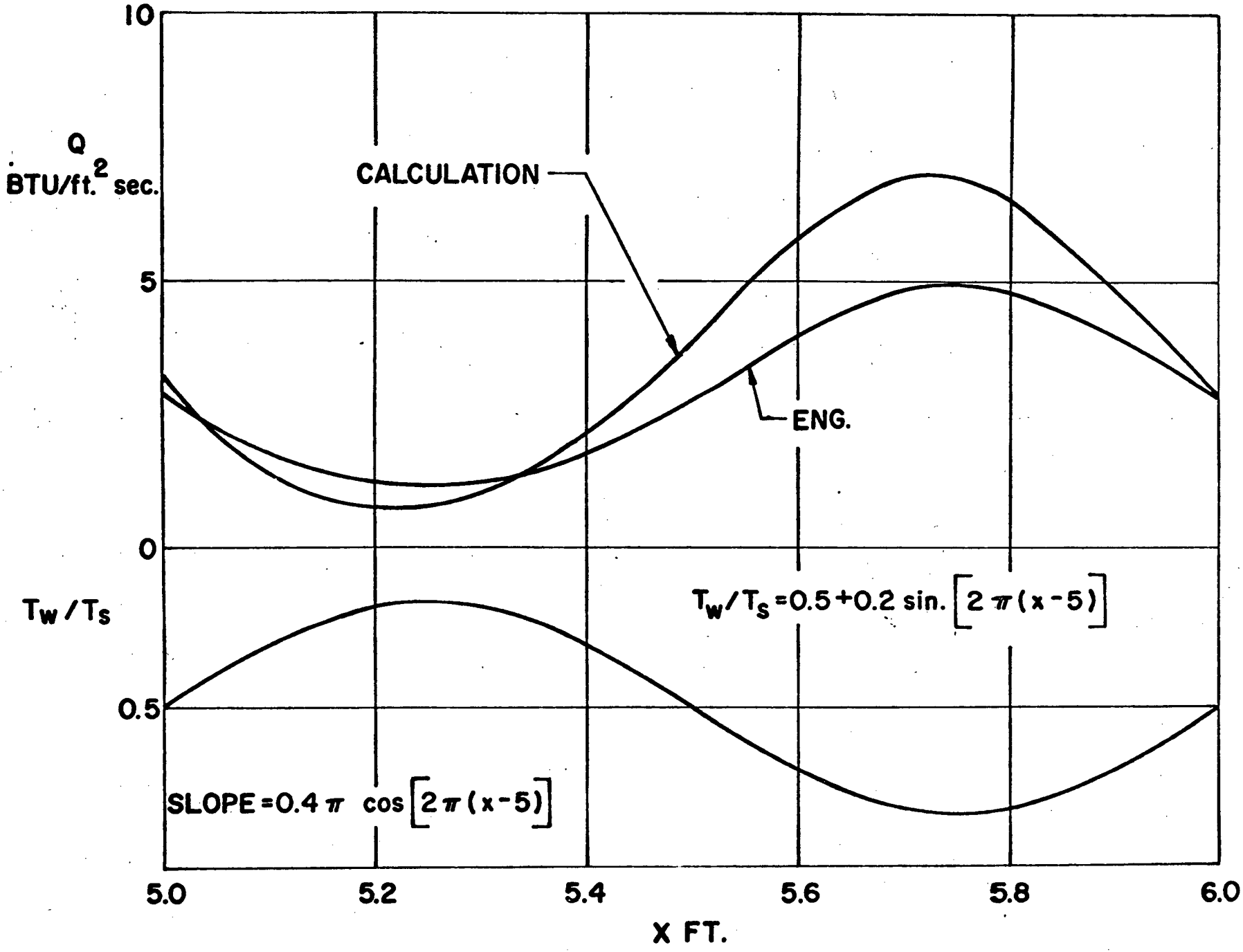

Fig. 18 Heat transfer distribution by numerical method

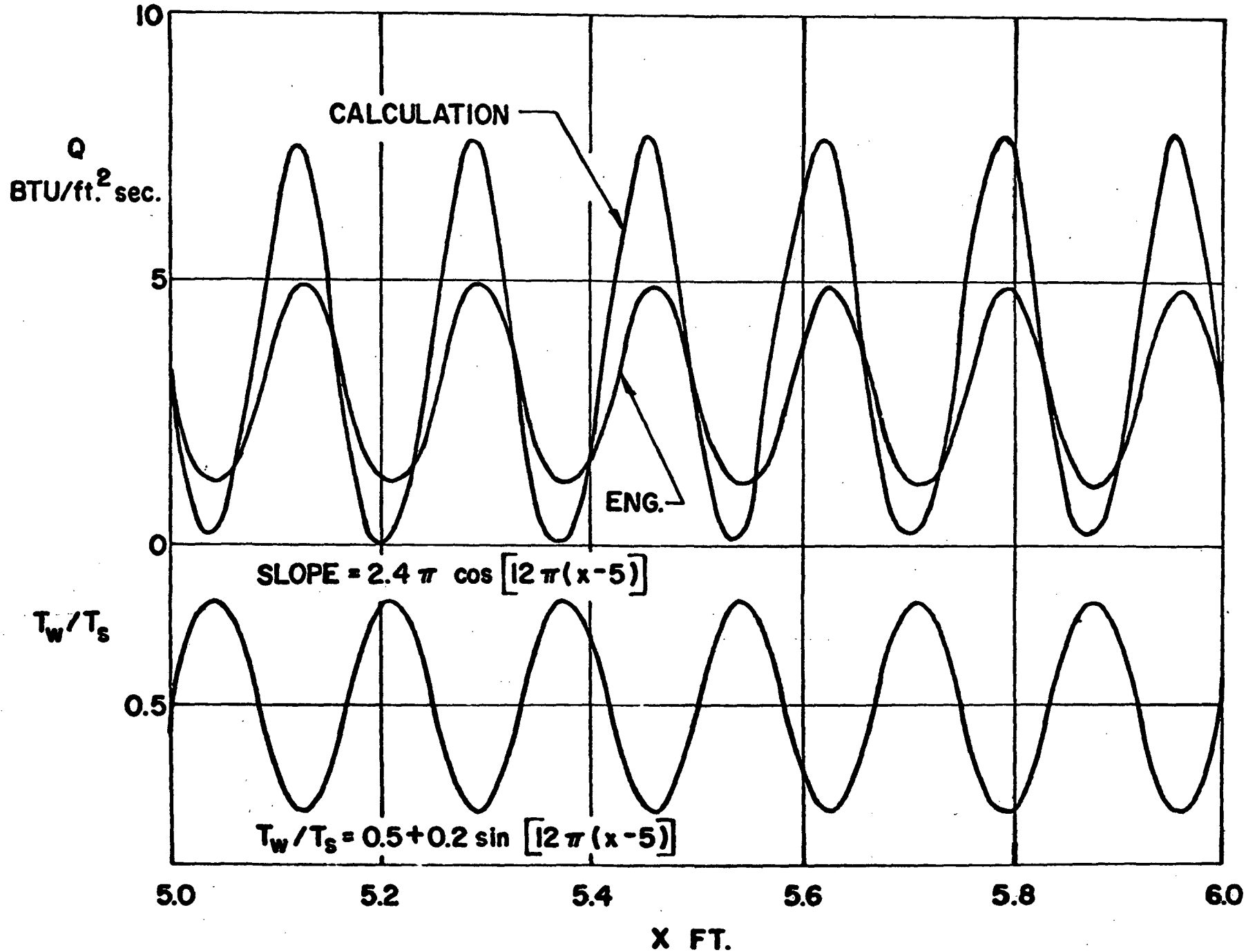

Fig. 19 Heat transfer distribution by numerical method